**Supporting Information**

# Highly hierarchical porous ultrathin $Co_3O_4$ nanosheets@Ni foam for high performance supercapacitors

Min Kang,[†] Hai Zhou,[*,†] Pushan Wen,[*,†] Ning Zhao[‡]

[†]Department of Chemistry and Chemical Engineering, Zunyi Normal college, Zunyi 563006, China

[‡]State Key Laboratory of Coal Conversion, Institute of Coal Chemistry, Chinese Academy of Sciences, Taiyuan 030001, China

E-mail: 591658314@163.com (Hai Zhou); wenpushan@126.com (Pushan Wen).

## Experimental

### Preparation of P-NiCoO-ns@NF, P-NiO-ns@NF, P-$Fe_2O_3$-ns@NF and P-$MnO_2$-ns@NF

The PVP mediated nanocomposites of P-NiCoO-ns@NF, P-NiO-ns@NF, P-$Fe_2O_3$-ns@NF and P-$MnO_2$-ns@NF were synthesized in the same manner to that of P-$Co_3O_4$-ns@NF. With the aim of preparing the above-mentioned four nanocomposites, the molar ratio of transitional metal nitrates to formamide was kept unchanged. Specially, 0.18g/0.12g $Co(NO_3)_2{\cdot}6H_2O$/$Ni(NO_3)_2{\cdot}6H_2O$, 0.3 g $Ni(NO_3)_2{\cdot}6H_2O$, 0.416 g $Fe(NO_3)_3{\cdot}9H_2O$, and 0.24 mL $Mn(NO_3)_2$ solution (50% wt. in $H_2O$) were used as the corresponding metal sources, respectively.

### Electrochemical measurements

After cutting into smaller pieces (ca. 1×1 $cm^2$), the as-prepared nanocomposites were used as the electrodes directly. The electrochemical properties of the nanocomposites were measured in a three-electrode cell on CHI660e (Chenhua, Shanghai, China) electrochemical workstation. Saturated calomel electrode (SCE), platinum plate electrode and the nanocomposites were used as the reference electrode, counter electrode and working electrode, respectively. 3 M KOH was used as electrolyte. The active carbon (AC) electrode was prepared in a similar way as described in literature.[1] The specific capacity ($C_s$, $C{\cdot}g^{-1}$) of nanocomposites was calculated by using the following equation:[2]

$$C_s = \frac{I \times \Delta t}{m} \qquad (1)$$

where $I$, $\Delta t$ and $m$ were the discharge current (A), discharge time (s) and mass of electroactive materials (g), respectively.

The specific capacitance ($C_{sc}$, $F \cdot g^{-1}$) of AC electrode was calculated by using equation (2):[3,4]

$$C_{sc} = \frac{I \times \Delta t}{m \times \Delta V} \qquad (2)$$

where $\Delta V$ was the potential window (V).

**Fabrication of P-$Co_3O_4$-ns@NF//AC asymmetric supercapacitor**

The P-$Co_3O_4$-ns@NF//AC asymmetric supercapacitor (ASC) was assembled by a P-$Co_3O_4$-ns@NF electrode and an AC (XFNANO, Nanjing, China) electrode with an NKK separator. 3 M KOH was also used as the electrolyte. To achieve the optimal electrochemical performance of the ASC device, the mass of active materials between the two electrodes was balanced according to equation (3), so as to ensure the balancing of charge between the two electrodes.[2]

$$\frac{m_+}{m_-} = \frac{C_{sc} \times \Delta V_-}{C_s} \qquad (3)$$

where $m_+$ and $C_s$ were the mass (mg) and specific capacity ($C \cdot g^{-1}$) of the P-$Co_3O_4$-ns@NF electrode, respectively, and $m_-$, $C_{sc}$ and $\Delta V_-$ were the mass (mg), specific capacitance ($F \cdot g^{-1}$) and potential window (V) of the AC electrode, respectively.

The specific capacitance ($C_{sc}$, $F \cdot g^{-1}$) of the ASC device was also calculated by equation (2) based on the total mass of active materials. The energy density ($E$,

Wh·kg$^{-1}$) and power density ($P$, W·kg$^{-1}$) of the device were calculated as follows:[2,3]

$$E = \frac{C_{sc} \times \Delta V^2}{7.2} \qquad (4)$$

$$P = \frac{3600 \times E}{\Delta t} \qquad (5)$$

where $C_{sc}$, $\Delta V$ and $\Delta t$ were the specific capacitance of ASCs, potential window (V) and the discharge time (s), respectively.

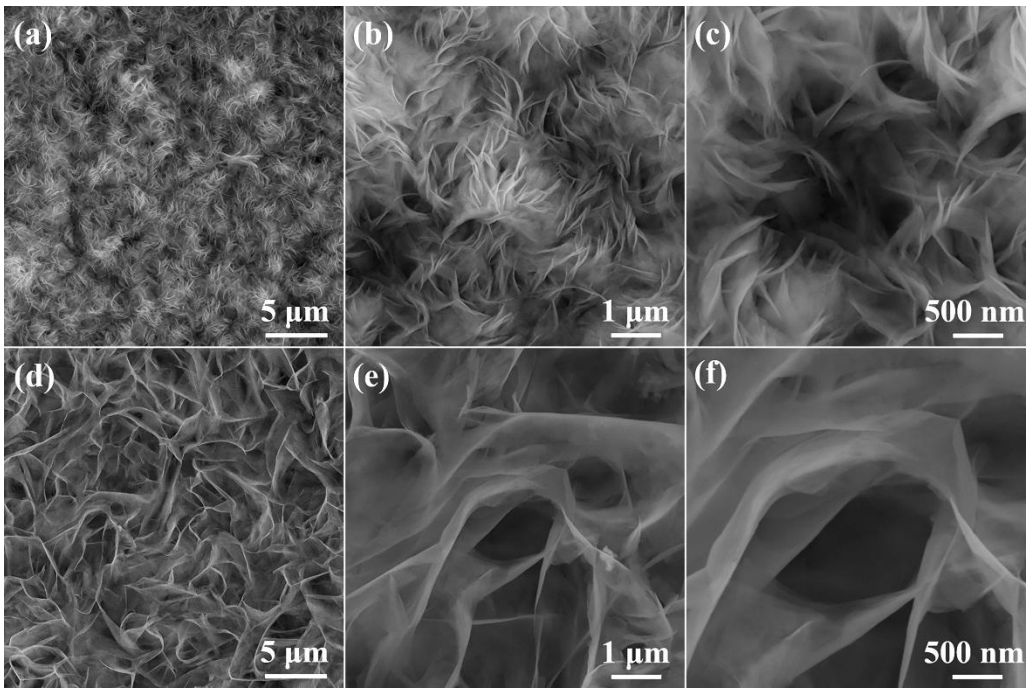


**Figure S1.** SEM images of the precursors for (a~c) P-$Co_3O_4$-ns@NF and (d~f) $Co_3O_4$-ns@NF.

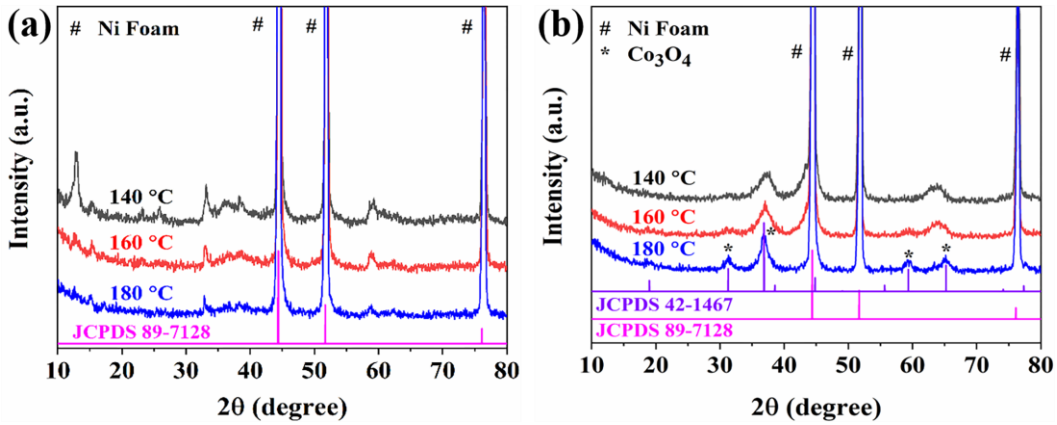


**Figure S2.** XRD patterns of (a) the PVP mediated precursors prepared at different temperatures and (b) the resulting nanocomposites.

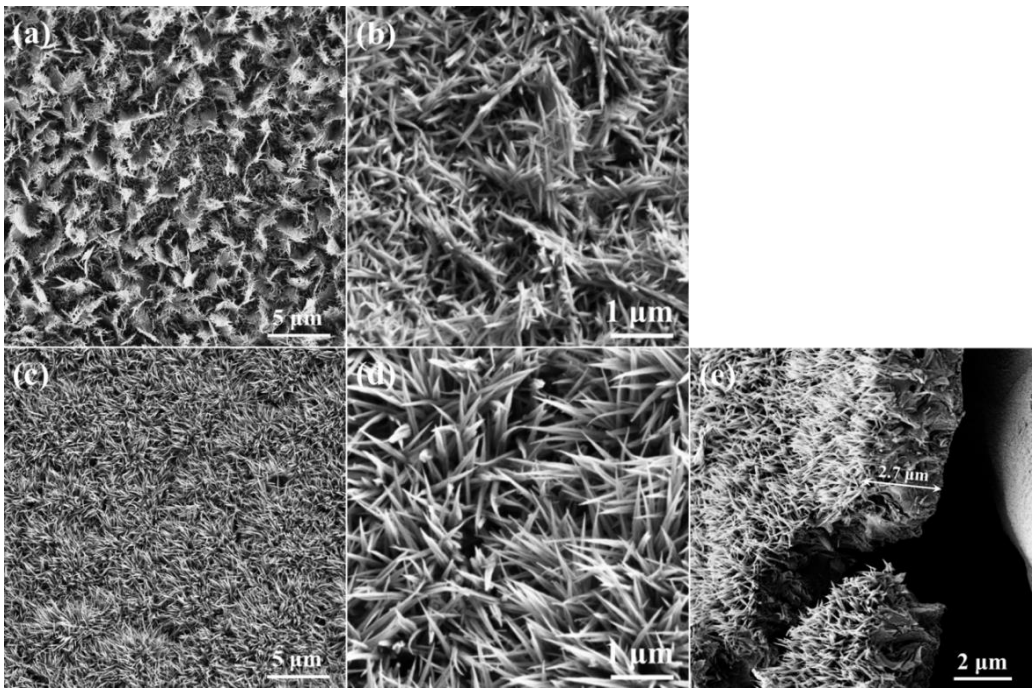


**Figure S3**. SEM images of nanocomposites obtained via the thermal annealing of precursors prepared at the hydrothermal temperatures of (a, b) 160 °C and (c~e) 180 °C (P-$Co_3O_4$-nw@NF) with the assistance of PVP.

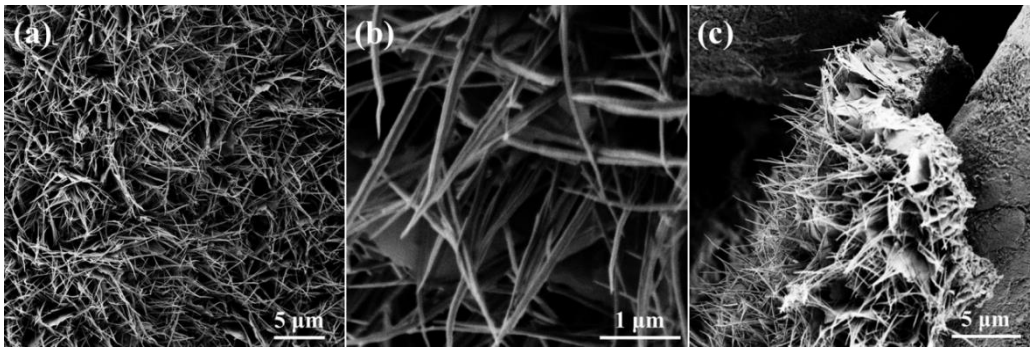


**Figure S4**. SEM images of (a~c) $Co_3O_4$-nw@NF obtained via the thermal annealing of precursor prepared at the hydrothermal temperature of 180 °C without the assistance of PVP.

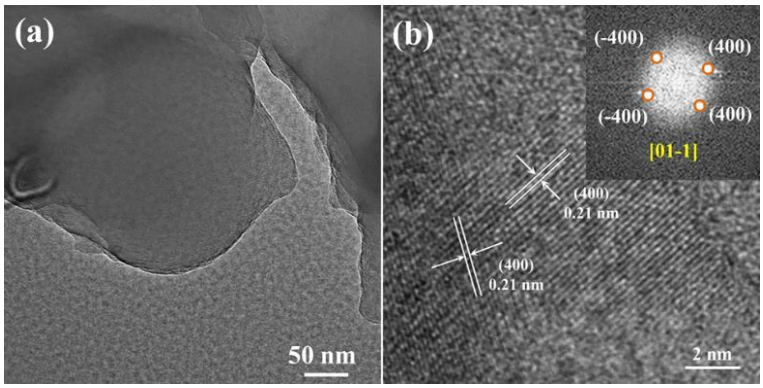


**Figure S5** (a) TEM and (b) HRTEM images of $Co_3O_4$ nanosheet scratched from $Co_3O_4$-ns@NF.

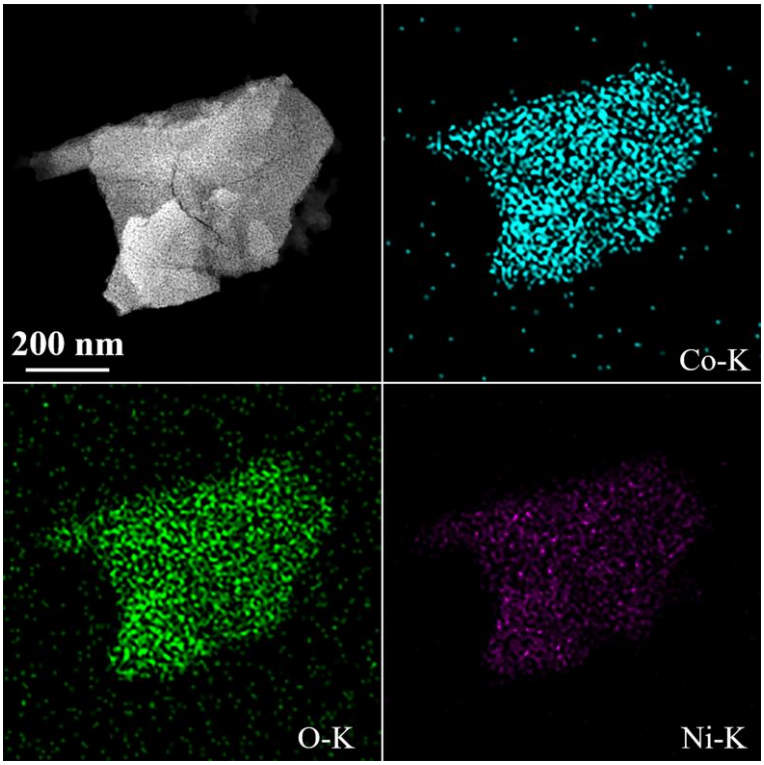


**Figure S6.** TEM image and TEM-mapping of P-$Co_3O_4$-ns@NF.

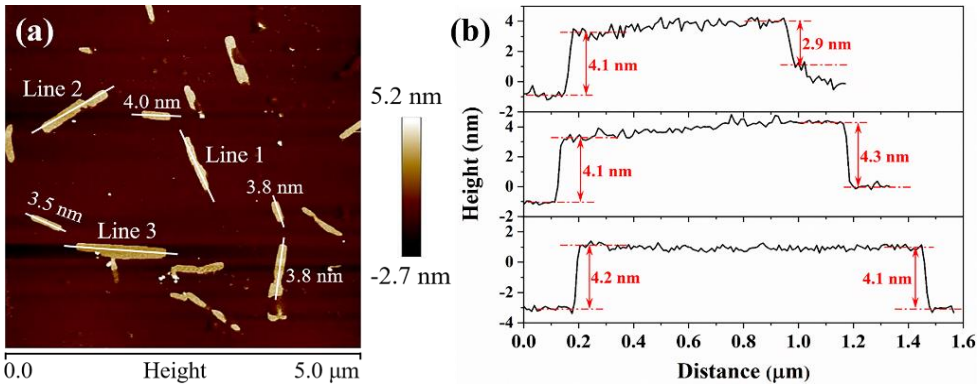


**Figure S7.** (a) AFM image of $Co_3O_4$ nanosheets scratched from $Co_3O_4$-ns@NF. (b) Height profiles derived from the marked lines in (a).

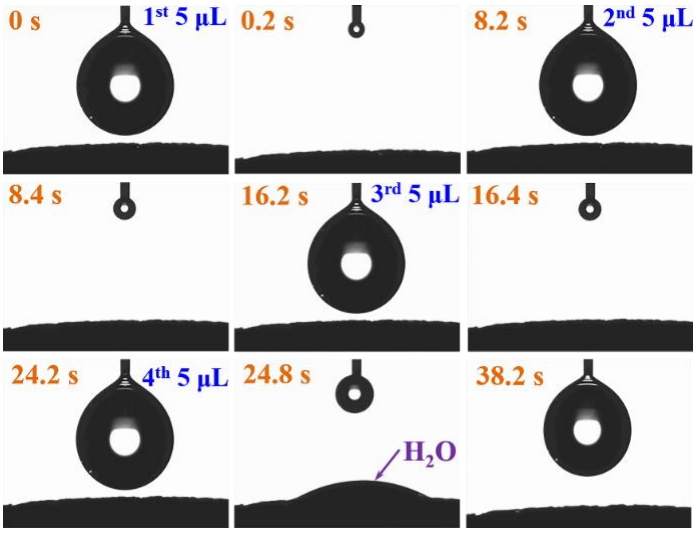


**Figure S8.** Wetting angles of water droplet on $Co_3O_4$-ns@NF.

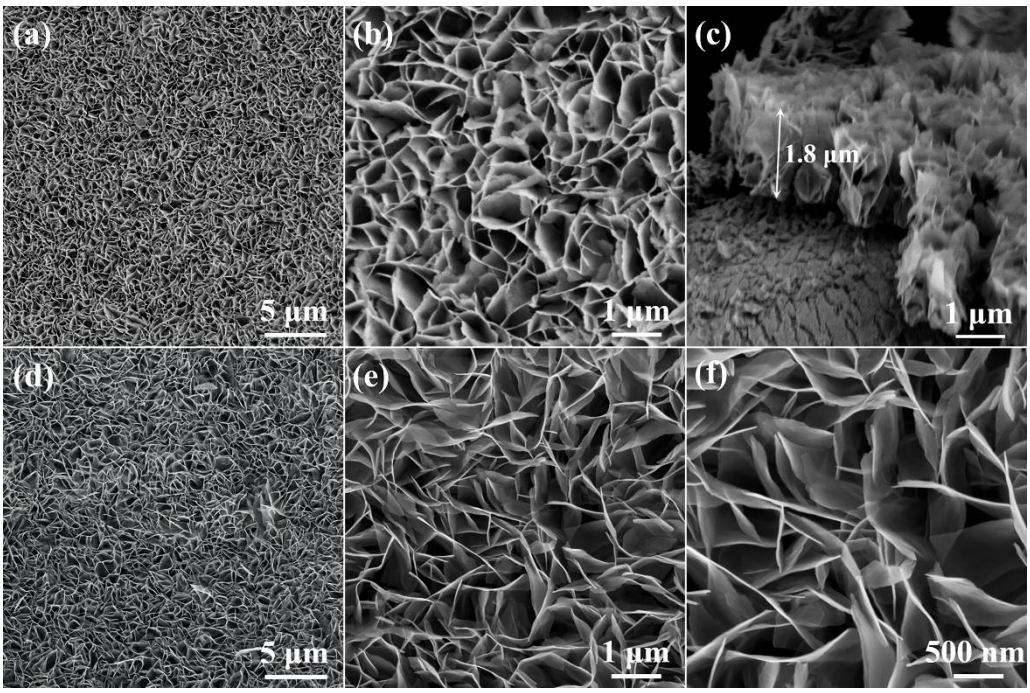


**Figure S9**. SEM images of (a~c) P-NiCoO-ns@NF and (d~f) P-NiO-ns@NF obtained via the thermal annealing of precursor prepared at the hydrothermal temperature of 140 °C with the assistance of PVP.

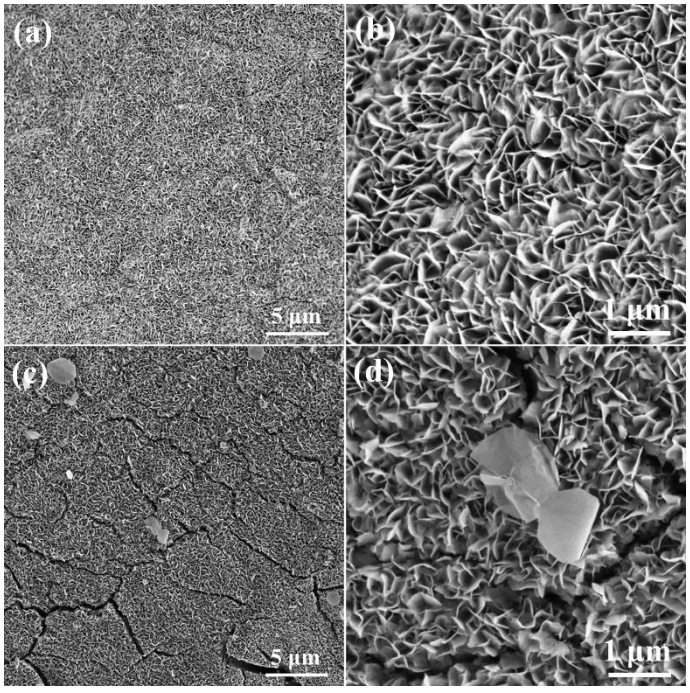


**Figure S10**. SEM images of (a, b) P-$Fe_2O_3$-ns@NF and (c, d) P-$MnO_2$-ns@NF obtained via the thermal annealing of precursor prepared at the hydrothermal

temperature of 140 °C with the assistance of PVP.

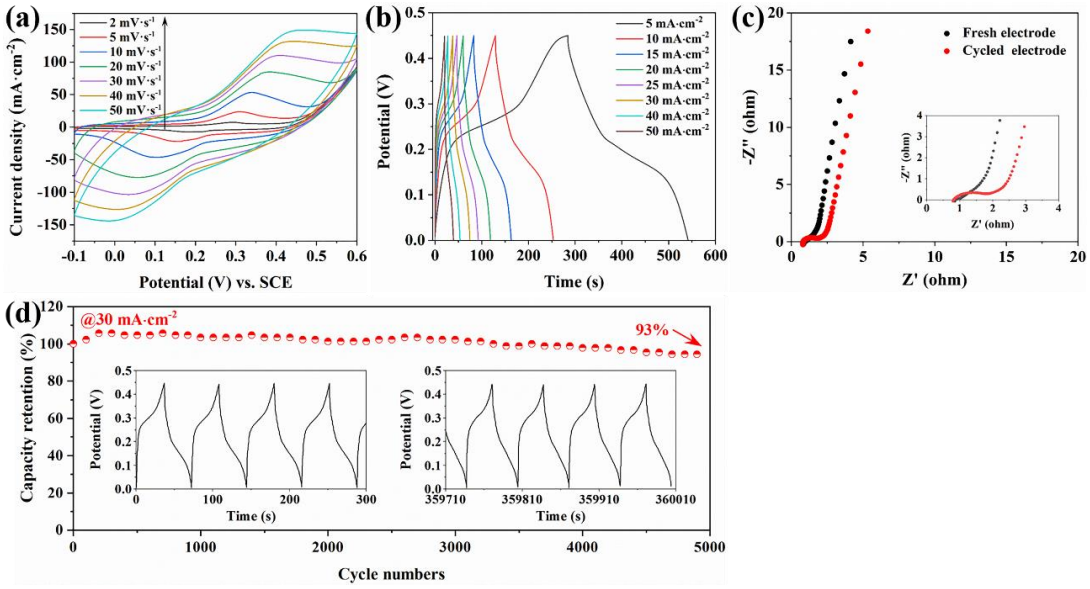


**Figure S11**. (a) CV and (b) GCD curves of $Co_3O_4$-ns@NF. (c) EIS curves of $Co_3O_4$-ns@NF before and after cycling test. (d) Cycling performance of $Co_3O_4$-ns@NF at 30 mA·cm$^{-2}$.

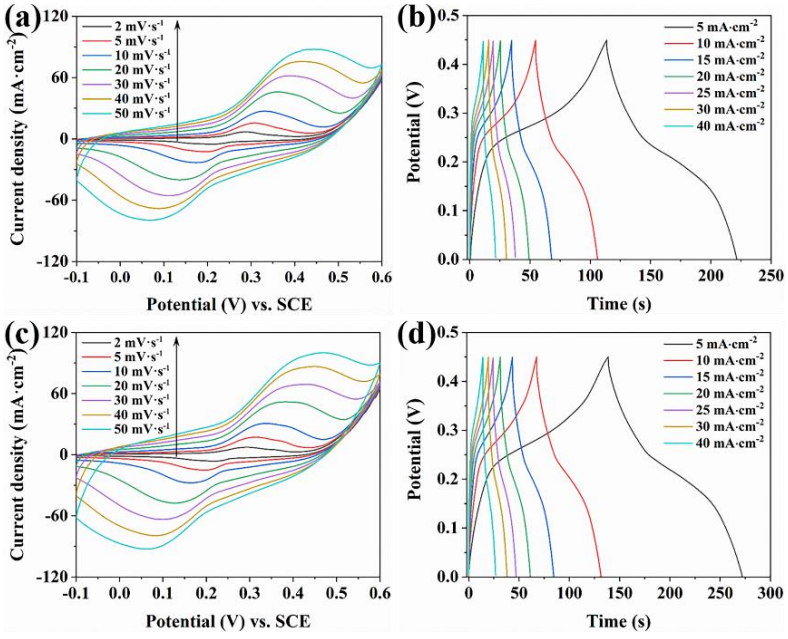


**Figure S12**. (a, c) CV and (b, d) GCD curves of P-$Co_3O_4$-nw@NF (top) and $Co_3O_4$-nw@NF (bottom).

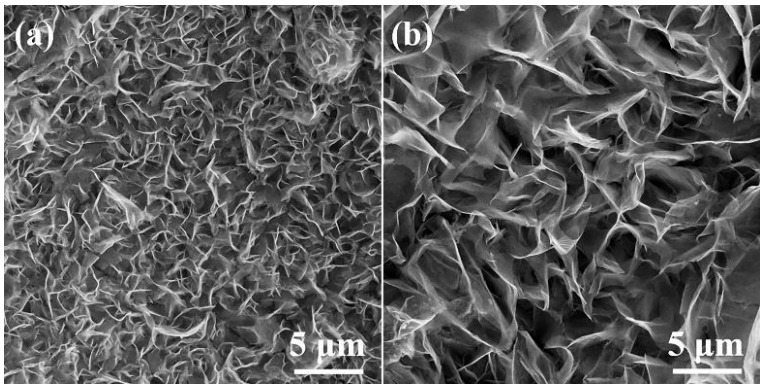


**Figure S13**. SEM images of (a) P-$Co_3O_4$-ns@NF and (b) $Co_3O_4$-ns@NF after cycling test.

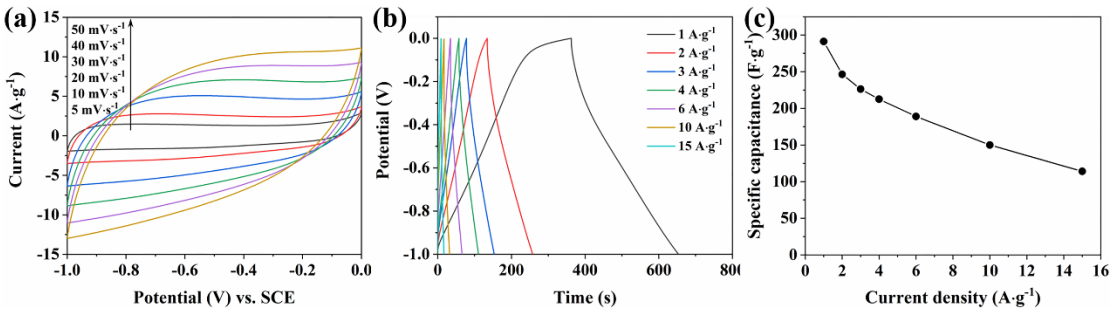


**Figure S14**. (a) CV curves, (b) GCD curves and (c) specific capacitance of the AC electrode. The specific capacitance of the AC electrode is 291.2, 246.4, 226.2, 212.4, 189, 150 and 114 F·$g^{-1}$ at 1, 2, 3, 4, 6,10 and 15 A·$g^{-1}$, respectively.

**Table S1.** Summary of electrochemical performance of cobalt oxides-based electrodes.

| Materials | Specific capacity/Current density | Capacity retention(%)/Cycles | Ref. |
|---|---|---|---|
| P-$Co_3O_4$-ns@NF (1.5 mg·$cm^{-2}$) | 1196.5 mC·$cm^{-2}$/5 mA·$cm^{-2}$ (798 C·$g^{-1}$/3.3 A·$g^{-1}$) | 107%/5000 | This work |
| $Co_3O_4$-ns@NF (1.62 mg·$cm^{-2}$) | 1287.5 mC·$cm^{-2}$/5 mA·$cm^{-2}$ (795 C·$g^{-1}$/3.09 A·$g^{-1}$) | 93%/5000 | This work |
| Phosphate ion functionalized $Co_3O_4$-ns@carbon cloth (0.56 mg·$cm^{-2}$) | 1030 C·$g^{-1}$/4.5 A·$g^{-1}$ | 85%/10000 | 5 |
| Ni/Co oxide@carbon nanosheets (4 mg·$cm^{-2}$) | 793 C·$g^{-1}$/1 A·$g^{-1}$ | 94.5%/10000 | 6 |
| $Co_8FeS_8$@NG (2 mg·$cm^{-2}$) | 755.7 C·$g^{-1}$/2 A·$g^{-1}$ | 96.1%/1000 | 7 |
| $Co_3O_4$@$NiCo_2O_4$@carbon fibers (3.01 mg·$cm^{-2}$) | 580 C·$g^{-1}$/1 A·$g^{-1}$ | 95.8%/6000 | 8 |
| $NiCo_2O_4$ nanowire@Ni foam (3.0 mg·$cm^{-2}$) | 580 C·$g^{-1}$/2 A·$g^{-1}$ | 95.7%/10000 | 9 |
| Reduced mesoporous $Co_3O_4$ nanowires | 488.5 C·$g^{-1}$/2 A·$g^{-1}$ | 90%/2000 | 10 |
| $Co_3O_4$ nanocube@$Co(OH)_2$ nanosheet (~5 mg·$cm^{-2}$) | 477.2 C·$g^{-1}$/1.2 A·$g^{-1}$ | 97.4%/6000 | 11 |
| $Co_3O_4$ nanopillar array@ multi-channeled porous carbon (~5 mg) | 440.5 C·$g^{-1}$/0.5 A·$g^{-1}$ | 94.5%/2000 | 12 |
| Hollow fluffy $Co_3O_4$ cages (2~3 mg) | 427 C·$g^{-1}$/1 A·$g^{-1}$ | ca. 150%/10000 | 13 |
| $Co_3O_4$/$NiCo_2O_4$ double-shelled nanocages (1 mg·$cm^{-2}$) | 408.2 C·$g^{-1}$/5 A·$g^{-1}$ | 92.5%/12000 | 14 |
| $Co_3O_4$/rGO/CNTs | 245.7 C·$g^{-1}$/2 A·$g^{-1}$ | 96%/2000 | 15 |
| $Co_3O_4$/rGO (~5 mg) | 244.8 C·$g^{-1}$/0.5 A·$g^{-1}$ | 55.7%/1500 | 16 |

**References**

(1) Xiao, Z.; Mei, Y.; Yuan, S.; Mei, H.; Xu, B.; Bao, Y.; Fan, L.; Kang, W.; Dai, F.; Wang, R.; Wang, L.; Hu, S.; Sun, D.; Zhou, H. Controlled Hydrolysis of Metal-Organic Frameworks: Hierarchical Ni/Co-Layered Double Hydroxide Microspheres for HighPerformance Supercapacitors. *ACS Nano* **2019**, *13*, 7024-7030.

(2) Liu, S.; Sankar, K. V.; Kundu, A.; Ma, M.; Kwon, J.-Y.; Jun, S. C. Honeycomb-Like Interconnected Network of Nickel Phosphide Heteronanoparticles with Superior Electrochemical Performance for Supercapacitors. *ACS Appl. Mater. Interfaces* **2017**, *9*, 21829-21838.

(3) Chen, C.; Zhang, N.; He, Y.; Liang, B.; Ma, R.; Liu, X. Controllable Fabrication of Amorphous Co-Ni Pyrophosphates for Tuning Electrochemical Performance in Supercapacitors. *ACS Appl. Mater. Interfaces* **2016**, *8*, 23114-23121.

(4) Mathis, T. S.; Kurra, N.; Wang, X.; Pinto, D.; Simon, P.; Gogotsi, Y. Energy Storage Data Reporting in Perspective-Guidelines for Interpreting the Performance of Electrochemical Energy Storage Systems. *Adv. Energy Mater.* **2019**, *9*, 1902007.

(5) Zhai, T.; Wan, L.; Sun, S.; Chen, Q.; Sun, J.; Xia, Q.Xia, H.; Phosphate Ion Functionalized $Co_3O_4$ Ultrathin Nanosheets with Greatly Improved Surface Reactivity for High Performance Pseudocapacitors. *Adv. Mater.* **2017**, *29*, 1604167.

(6) Xiang, C.; Liu, Y.; Yin, Y.; Huang, P.; Zou, Y.; Fehse, M.; She, Z.; Xu, F.; Banerjee, D.; Merino, D. H.; Longo, A.; Kraatz, H.-B.; Brougham, D. F.; Wu, B.; Sun, L. Facile Green Route to Ni/Co Oxide Nanoparticle Embedded 3D Graphitic Carbon Nanosheets for High Performance Hybrid Supercapacitor Devices. *ACS Appl. Energy*

*Mater.* **2019**, *2*, 3389-3399.

(7) Haj, Y. A.; Balamurugan, J.; Kim, N. H.; Lee, J. H. Nitrogen-doped graphene encapsulated cobalt iron sulfide as an advanced electrode for highperformance asymmetric supercapacitors. *J. Mater. Chem. A* **2019**, *7*, 3941-3952.

(8) Wu, X.; Han, Z.; Zheng, X.; Yao, S.; Yang, X.; Zhai, T. Core-shell structured $Co_3O_4$@$NiCo_2O_4$ electrodes grown on flexible carbon fibers with superior electrochemical properties. *Nano Energy* **2017**, *31*, 410-417.

(9) Qiu, W.; Xiao, H.; Yu, M.; Li, Y.; Lu, X. Surface Modulation of $NiCo_2O_4$ Nanowire Arrays with Significantly Enhanced Reactivity for Ultrahigh-Energy Supercapacitors. *Chem. Eng. J.* **2018**, *352*, 996-1003.

(10) Wang, Y.; Zhou, T.; Jiang, K.; Da, P.; Peng, Z.; Tang, J.; Kong, B.; Cai, W.; Yang, Z.; Zheng, G. Reduced Mesoporous $Co_3O_4$ Nanowires as Efficient Water Oxidation Electrocatalysts and Supercapacitor Electrodes. *Adv. Energy Mater.* **2014**, *4*, 1400696.

(11) Pang, H.; Li, X.; Zhao, Q.; Xue, H.; Lai, W.-Y.; Hu, Z.; Huang, W. One-pot synthesis of heterogeneous $Co_3O_4$-nanocube/$Co(OH)_2$-nanosheet hybrids for high-performance flexible asymmetric all-solid-state supercapacitors. *Nano Energy* **2017**, *35*, 138-145.

(12) Zheng, Y.; Li, Z.; Xu, J.; Wang, T.; Liu, X.; Duan, X.; Ma, Y.; Zhou, Y.; Pei, C. Multi-channeled hierarchical porous carbon incorporated $Co_3O_4$ nanopillar arrays as 3D binder-free electrode for high performance supercapacitors. *Nano Energy* **2016**, *20*, 94-107.

(13) Zhou, X.; Shen, X.; Xia, Z.; Zhang, Z.; Li, J.; Ma, Y.; Qu, Y. Hollow Fluffy $Co_3O_4$ Cages as Efficient Electroactive Materials for Supercapacitors and Oxygen Evolution Reaction. *ACS Appl. Mater. Interfaces* **2015**, *7*, 20322-20331.

(14) Hu, H.; Guan, B.; Xia, B.; Lou, X. Designed Formation of $Co_3O_4$/$NiCo_2O_4$ Double-Shelled Nanocages with Enhanced Pseudocapacitive and Electrocatalytic Properties. *J. Am. Chem. Soc.* **2015**, *137*, 5590-5595.

(15) Yuan, C.; Yang, L.; Hou, L.; Li, J.; Sun, Y.; Zhang, X.; Shen, L.; Lu, X.; Xiong, S.; Lou, X. Flexible Hybrid Paper Made of Monolayer $Co_3O_4$ Microsphere Arrays on rGO/CNTs and Their Application in Electrochemical Capacitors. *Adv. Funct. Mater.* **2012**, *22*, 2560-2566.

(16) Song, Z.; Zhang, Y.; Liu, W.; Zhang, S.; Liu, G.; Chen, H.; Qiu, J. Hydrothermal synthesis and electrochemical performance of $Co_3O_4$/reduced graphene oxide nanosheet composites for supercapacitors. *Electrochimica Acta* **2013**, *112*, 120-126.